Compressive Sensing Based Data Acquisition Architecture for Transient Stellar Events in Crowded Star Fields

Asmita Korde-Patel
Goddard Space Flight Center,
NASA,
Greenbelt, MD, USA
University of Maryland, Baltimore County
Baltimore, MD, USA
asmita.a.korde@nasa.gov

Richard K. Barry
Goddard Space Flight Center,
NASA,
Greenbelt, MD, USA
richard.k.barry@nasa.gov

Tinoosh Mohsenin
University of Maryland, Baltimore County
Baltimore, MD, USA
tinoosh@umbc.edu

***Abstract*—Compressive sensing (CS) is a mathematical technique for simultaneous data acquisition and compression. In this work, we show a CS based architecture for acquiring and reconstructing transient astrophysical events. This architecture reconstructs a differenced image, eliminating the need for any sparse domain transforms, otherwise required for traditional CS reconstruction. The resulting reconstructed differenced image is of importance as the information required for generating time-series photometric light curves is best obtained from an image differenced with a reference image. This architecture eliminates the need to 1.) transform an image to a sparse domain, 2.) reconstruct a dense field, and then apply differencing on the image to obtain the time-ordered photometry. We study the case of gravitational microlensing in which a distant source star in a crowded field is briefly magnified by the passage of a mass through the line of sight between the source star and observer. Our results show that this architecture is able to reconstruct the light curve for magnification factors greater than 1 with error less than 2% using only 10% of the Nyquist rate samples.**

***Index Terms*—Compressive Sensing, Data acquisition, Image differencing, Gravitational microlensing, Transient photometry**

I. Introduction

Miniaturization is a dominant new trend in astronomical mission development. While small space observatories offer an exciting low-cost approach to obtaining measurements, such spacecraft are typicality power limited due to available solar array area. Among other considerations, this has the effect of placing a hard limit on the distance a small satellite may be from its receiver due to communications power requirements. Could CS be profitably employed to reduce telecommunications bandwidth? What are the implications for the science? Would systematics associated with the process significantly impact the information in the data? Here we seek to directly assess these questions for the case of a rapidly fluctuating source star in a crowded field.

Here we describe the application of CS to remotely sensed time-ordered photometric measurements, specifically stars undergoing magnification due to the passage of a mass in the intervening space - a phenomenon known as gravitational microlensing. Microlensing events are exceedingly rare thus requiring wide-field imaging of very dense stellar fields for detection. As a consequence, microlensing light curves are typically extracted using optimal image subtraction rather than aperture photometry or point-spread function fitting photometry. A difference image is created by subtracting a reference image from the observed image using a convolution kernel. Differencing and its implications for microlensing are provided in Section III. The pertinent information required to generate a microlensing curve, which in turn, gives information about the lensing body, is obtained through the differenced image. Importantly, retaining the observed dense spatial image is not essential for the acquisition of the microlensing signal. In this paper, we present a novel CS architecture which applies optimal image subtraction to the CS measurements themselves, and reconstructs the differenced image as required for microlensing applications. We begin with a brief background on microlensing and compressive sensing, followed by the architecture implementation description. Finally, we show simulation results, and discuss a summary of the results in the Conclusions section.

II. Gravitational Microlensing

There are many sources of stellar variability that are of interest to the astronomical community. Imaging data and extracted photometric light curves can take an extraordinary variety of forms with very subtle features. The features may be studied to understand the underlying astrophysical processes. One such source of stellar variability that is particularly apt for the assessment of the application of CS is gravitational microlensing.

Gravitational microlensing is a phenomenon that occurs due to the chance alignment of a distant source star, the observer and a mass in the intervening space. The mass warps space-time, causing the light traveling radially away from the source star to bend inward towards the mass thus following the path of least time. Images of the source star are created by the

978-1-7281-4460-3/20/$31.00 ©2020 IEEE

lensing mass with the ratio of the area of the images to the apparent area of the source star defined as the magnification. Flux is conserved in this process, and, as a consequence, the magnification is manifested as a change in the source star's brightness. The rate of change of brightness of the source is proportional to the rapidity of apparent motion of the source relative to the lensing mass. If a planetary companion of the lensing star happens to pass through one of the lensed images of the source, the magnified light from the source will exhibit an inflection [1].

The alignment of the source, lensing mass and the observer must be exquisitely precise to result in significant magnification. The amount of magnification varies inversely with the impact parameter of source and lens, dropping rapidly as it exceeds the lens' Einstein ring radius. The Einstein ring radius varies as the square root of the ratio of the Schwarzschild radius, $r_s = 2GM/c^2$, of the lens and the relative lens-source distance. For the typical case of a source star in the Galactic bulge at a distance of about 8 kpc and a $\sim$ 0.3 solar mass M5 dwarf lens star at 4 kpc, the alignment of source, lens and observer, measured by the impact parameter, would need to be less than 300 pico-radians on the sky to yield a magnification greater than 10 - *exquisitely* precise. The consequence of this constraint is that measurable microlensing events are exceedingly rare thus requiring a high density of stellar sources to permit a reasonable event rate. Detection of a planetary companion to a lensing star is even more rare with a vanishingly small probability of occurrence outside of the very densest stellar fields. This makes the phenomenology of gravitational microlensing an ideal laboratory to study the systematic behavior of CS for crowded images.

III. Difference Imaging

Stellar images are differenced in order to retain only the star sources experiencing a changing in magnification. Differencing is performed by obtaining a convolution kernel which matches the point spread function (PSF) of a reference image to that of an observed image, and then performs subtraction using the matched image [2].

$$x_{diff} = (x_o - (x_r \star K)) \tag{1}$$

where x_{diff} is the differenced image, x_o is the observed image, x_r is the reference image, and K is the convolution kernel. In our work, we represent $\star$ as a convolution operator. x_o can be defined as

$$x_o = x_s \star P_O \tag{2}$$

and x_r can be define as

$$x_r = x_s \star P_R \tag{3}$$

where x_s represents a spatial region and P_O and P_R are the detector responses as given by the PSF functions for x_o and x_r, respectively. In our simulations we use a Gaussian function spread to define the PSF of both the observed and reference images. A reference image has a cleaner PSF, that is, the spread of a point source due to the detector's response is very narrow. This is usually generated by registering good seeing images. Detector optics along with other atmospheric factors determine the detector seeing, which in turn is characterized by the PSF. An observed image in our context is any image output of a detector system, typically with a worse seeing PSF as compared to a reference image. In this work, we refer to good seeing images as images produced with a narrow spread PSF. From hereon, the PSF value can be inferred as the standard deviation of a Gaussian kernel in both x and y direction in pixel units for 2D images. The PSF of the observed and reference image can have a great impact on the effects of CS on the resulting differenced image.

IV. Compressive Sensing Background

Compressive sensing is a mathematical theory for sampling at a rate much lower than the Nyquist rate, and yet, reconstructing the signal back with little or no loss of information. The signal is reconstructed by solving an underdetermined system. This works only when the signal we are solving for is sparse in the domain we are reconstructing. Hence, if it is not sparse in the sampling domain, we can transform it to a sparse domain, perform the reconstruction and then transform it back to the original domain.

We assume x to be k-sparse signal of length n. A is the measurement matrix and is of size m x n. The acquired measurements vector, y, therefore, is of length m. These dimensions are for 1D signals. Extension to 2D images are discussed in Section V. A signal whose coefficients decay at a high rate is sparse [3]. Hence, in an image, pixel values which have similar ranging values for all, but k pixels, is said to be k sparse, where the k pixels have significantly higher values.

In a CS system, we collect m measurements, where $m << n$. Using the acquired measurements vector y and the known measurement matrix A, we can reconstruct x using various L_1 norm minimization reconstruction algorithms to obtain a sparse x [4] [5] [6]. Various reconstruction algorithms are discussed in [7]. We solve for equation (4) to determine x through the observation y.

$$y = Ax \tag{4}$$

In this work, we use a conic optimization algorithm provided by [8] [9] to solve for our signal of interest.

V. Compressive Sensing Architecture

In this paper, we discuss a novel CS-based architecture for acquiring differenced crowded stellar images. Our research is targeted towards microlensing events, however, it can be extended to any astronomical events which require differenced images for observing transient events. Our previous work ([10], [11]) shows optimistic preliminary results for applying CS to very sparse spatial images consisting of a star source experiencing single lens microlensing event. This research extends to differenced images by applying a novel CS architecture. Figure 1 shows how CS is used as a data acquisition technique to obtain a photometric light curve.

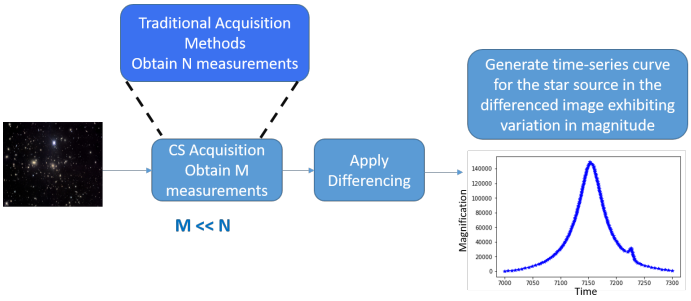

Fig. 1. CS Implementation overview

A traditional CS based architecture will use a sparse domain transform ϕ, to sparsify the crowded stellar field [12] [13], which would then be reconstructed using optimization techniques. The architecture overview is shown in Figure 2.

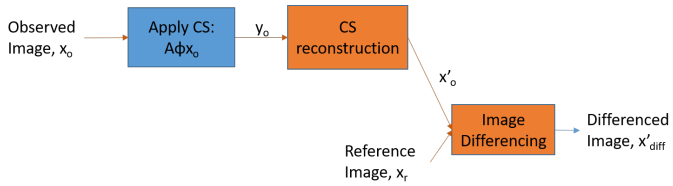

Fig. 2. Traditional CS Architecture for acquiring differenced images
blue: on-board processing, orange: ground processing

In this work, we demonstrate a CS based architecture for efficiently obtaining only the transient star sources in crowded stellar fields. Applying this technique to differenced images over time can help generate the light curve shown in Figure 1. This architecture, shown in Figure 3, implements differencing at the CS measurement level. The output of this architecture is a differenced image. Thus, the original spatial sky image is not preserved. We study limitations and requirements of this architecture. The architecture is implemented in the following

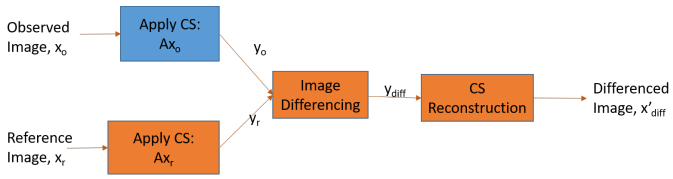

Fig. 3. CS Architecture implementing differencing during CS reconstruction
blue: on-board processing, orange: ground processing

manner:

1) Obtain CS based measurements, y_o for a spatial image. CS can be applied by projecting a matrix, A onto the region of interest, x_o. This can be done on a column-by-column basis for a n x n spatial region, x_o. Thus, for 2D images, y_0 and A are of size m x n, where $m << n$.
2) Given A and a clean reference image, x_r, construct measurements matrix y_r, where $y_r = Ax_r$
3) Apply a 2D differencing algorithm on y_o and y_r to obtain a differenced image, y_{diff}, and the corresponding convolution kernel, M, which is used to match the observed and reference CS measurement vectors, y_o and y_r .
4) Reconstruct the differenced image, x'_{diff} using CS algorithms, given A and y_{diff}.

This architecture eliminates the need for sparsifying data as needed by traditional CS architectures since the reconstructed differenced signal would be sparse. This can reduce computational power and memory required for transforming into a sparse domain. As the measurements have a smaller dimension than the reconstructed images, computational power can also be reduced while differencing.

In this architecture, we create the differenced measurements matrix, y_{diff} by

$$y_{diff} = y_o - (y_r \star M) \tag{5}$$
$$= Ax_o - (Ax_r \star M) \tag{6}$$

Here x_o and x_r are the observed and reference images, respectively, and M is the obtained convolution kernel using differencing algorithm. The known parameters are A, y_o and x_r. Using differencing algorithms, we solve for M, to obtain y_{diff}.

For 2D images, if differencing gives optimal results, y_{diff} will have non-zero values in only the columns corresponding to the non-zero elements in x_{diff}. Hence, reconstructing y_{diff} using CS reconstruction techniques will give a sparse signal back, corresponding to x'_{diff}. To obtain the best results using CS techniques, $x'diff$ has to be very sparse. Sparsity of $x'diff$ in this case is dependent on two factors:

1) PSF: Images with fairly narrow PSFs, and reference and observed images which have a similar distribution PSF, give optimal results using differencing algorithms. This in turn, produces sparser differenced images. If the PSFs are able to be matched perfectly using a differencing algorithm, the differenced image will only contain center pixels with magnitude difference between the two.
2) Magnification: Sparsity in CS can also be viewed as the rate at which the coefficients decay [3]. The higher the rate of decay of the coefficients, the sparser the image. Hence, higher magnification events give a sparser image compared to lower magnification events. When magnification factor is 1, ideal differencing should result in zero magnitude over all pixels. In the case of all zero magnitude pixels, the sparsity is zero. This can lead to erroneous results as the CS reconstruction algorithm searches for k non-zero pixel values.

We want to solve for x'_{diff} as this is the differenced image, which contains pertinent information for generating a microlensing light curve. In our simplified case study, we study the effects of magnification of a source star, depicting a time sample of the microlensing light curve. Magnification at the source star with position $[p_1, p_2]$ is defined as

$$x_o[p_1, p_2] = mf(x_s[p_1, p_2]) \star P_O \tag{7}$$

where mf is the magnification factor, ranging from 1 to 1.8 in our experiments.

$$y_{diff} = A(x_{diff}) \tag{8}$$

In equation (8), $x_{diff} = x_o - (x_r \star K)$.

where $\delta - \epsilon \leq K \leq \delta + \epsilon$, and δ is defined by equation (9). For equation (10) to hold true, ϵ must be 0. For small quantities of ϵ, the results are discussed in section VI.

$$\int_{t_0 a}^{t_0 b} \int_{t_1 a}^{t_1 b} \delta(t_0, t_1) dt = \begin{cases} 1, & \text{if } t_0 = p_1, t_1 = p_2 \\ 0, & \text{otherwise} \end{cases} \tag{9}$$

where $t_0 a < t_0 < t_0 b$ and $t_1 a < t_1 < t_1 b$

If $\epsilon = 0$, then

$$Ax_o - (Ax_r \star M) = A(x_o - (x_r \star K)) \tag{10}$$

In practical cases, differencing algorithms like Difference Image Analysis (DIA) are used to find this kernel given two images. Although a differenced image with no microlensing events will give sub-optimal results, an image with a microlensing event should increase image sparsity leading to better CS reconstruction results. We use a conic optimization algorithm as described in [8] [9] to solve the optimization problem shown in equation (11).

$$\begin{aligned} &\text{minimize } ||x'_{diff}||_1 \text{ s.t.} \\ &(Ax'_{diff} - y_{diff}) \leq 0.001 \end{aligned} \tag{11}$$

VI. Simulation Results

Using the proposed CS based architecture for 2D images, we apply CS on a column-by-column basis for a 2D spatial crowded stellar field. We use a 128x128 size image with 128 star sources spread across spatially in a random uniform manner. The flux of these star sources are also generated uniform randomly within the range of $[10000, 50000]$ units of pixel magnitude. Figure 4 and Figure 5 show a clean reference image and an observed image with a worse seeing PSF, respectively. For CS, a Gaussian normal random measurement matrix is applied. We analyze the average $\%$ error and standard deviation of the error over 100 Monte Carlo simulations, where the random Gaussian measurement matrix is varied. Given the CS architecture described in section V, we reconstruct a differenced image, and then analyze the accuracy in reconstruction of the microlensing photometric curve over time. The reconstructed result (sample image shown in Figure 7) is compared to that of the differenced image resulting from applying DIA on the spatial domain images, x_o and x_r (sample image shown in Figure 6). Statistical error analysis using varying parameters is shown in tables I, II, III, and IV. As DIA is the current state-of-art differencing algorithm, we use that as our basis for comparison. The % error is calculated by

$$\frac{|x'[s_0, s_1] - x[s_0, s_1]|}{x[s_0, s_1]} \times 100\% \tag{12}$$

Here, s_0 and s_1 are pixel indices corresponding to the center pixel of the star experiencing a change in flux. $x[s_0, s_1]$ is the DIA output value at position $[s_0, s_1]$. Similarly $x'[s_0, s_1]$ is the reconstructed differenced image value at position $[s_0, s_1]$.

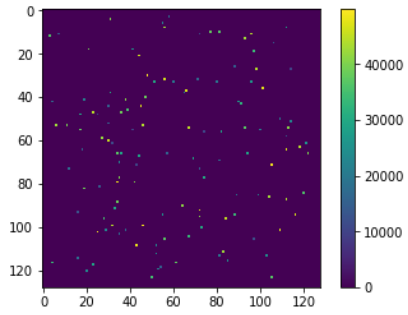

Fig. 4. Reference Image with 0.1 pixel units standard deviation PSF

Simulations are performed for a reference image with a PSF of 0.1 pixel units of standard deviation for a Gaussian spread PSF in both x and y direction. Similarly, the observed image has a PSF with standard deviation of 0.1, 0.3 or 0.5 pixel units. In table I, the PSF of the reference image is 0.1 pixel units and PSF of observed image is 0.3 pixel units. In this case, the kernel is known a-priori. Hence, in equation (6), M is known. Magnification factor is used to calculate the amplification value of the source star at position $[s_0, s_1]$:

Amplification Value = Source star value x magnification factor

When the magnification factor is 1, there is no change in the magnification of the source star. Hence, the resulting differenced image should have ideally all zero value pixels if the differencing works perfectly. However, for CS to give optimal results, the differenced image must be sparse, that is, the coefficients in the differenced image must decay at a high rate, which is not the case if all of the pixel values are close to zero. This results in the higher $\%$ error when there is no change in magnification (magnification factor = 1).

We show that for when the observed image PSF is similar in characteristics as the reference image PSF, the error in CS

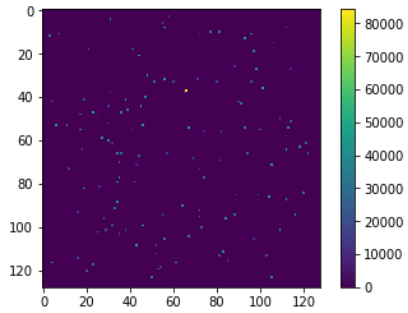

Fig. 5. Observed Image with 0.3 pixel units standard deviation PSF

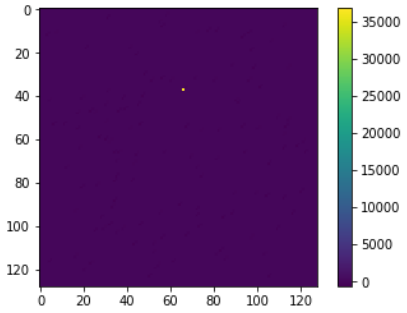

Fig. 6. Residual after differencing using DIA

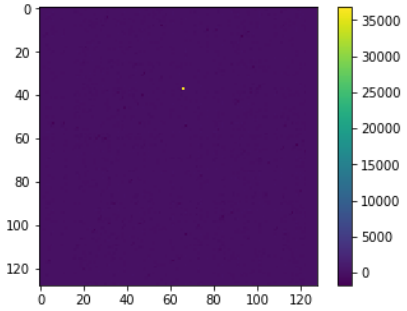

Fig. 7. Reconstructed residual using CS techniques with 10% of Nyquist rate measurements

reconstruction is significantly lower. A summary plot is shown in Figure 8. The legends are described in table V.

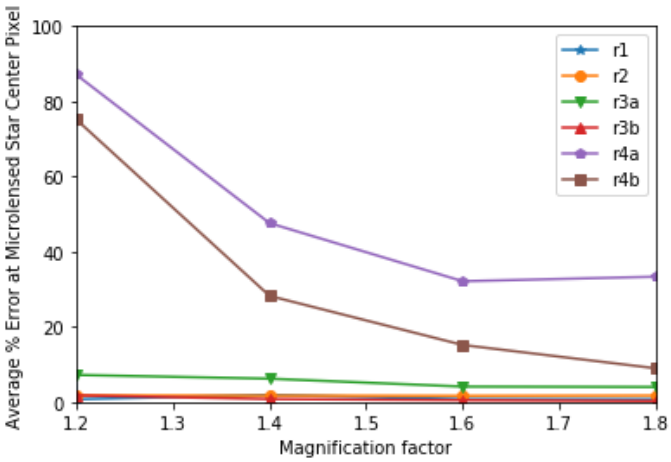

Fig. 8. Average % Errors for the configureations shown in table V

From the results it is evident that when no magnification takes place, the differenced image is not sparse, hence, CS does not work well. A 100% error indicates a false positive, that is, the differenced image value of the pixels indicating the presence of the source star is zero, but a non-zero value is detected. However, as magnification factor increases, CS results give minimal error. This architecture gives optimal results in either of three circumstances, given a transient event

TABLE I
AVERAGE % ERROR IN MAGNITUDE OF THE SOURCE STAR AND STANDARD DEVIATION OF ERROR OVER 100 MONTE CARLO SIMULATIONS. CONVOLUTION KERNEL, M IS KNOWN. OBSERVED IMAGE PSF = 0.3 REFERENCE IMAGE PSF = 0.1

Magnification Factor	Average % error	standard deviation of error
1	100	0.093
1.2	0.73	0.0073
1.4	1.87	0.099
1.6	0.75	0.0077
1.8	0.73	0.0072

TABLE II
AVERAGE % ERROR IN MAGNITUDE OF THE SOURCE STAR AND STANDARD DEVIATION OF ERROR OVER 100 MONTE CARLO SIMULATIONS. OBSERVED IMAGE PSF = 0.1 REFERENCE IMAGE PSF = 0.1.

Magnification Factor	Average % error	standard deviation of error
1	100+	1244
1.2	1.75	0.0090
1.4	1.70	0.0097
1.6	1.64	0.0090
1.8	1.71	0.0090

is taking place:

1) Convolution kernel for differencing is known a-priori
2) PSF of an observed image has similar characteristics as the reference image PSF
3) There is a significant change in magnification of a star source experiencing a transient event

If these requirements are not met, the number of measurements can be increased to reduce the error. Table IV, shows how the error can be drastically reduced by increasing the number of measurements from 10% of n to 50% of n. In cases where the ratio of PSF of the reference image to observed image is $1:5$ for a magnification factor of 1.8, the error is reduced to less than 10% with 50% measurements.

Furthermore, it is evident that CS techniques can work within 10% accuracy using only 10% of the required samples for crowded stellar fields when both the reference and observed image have fairly narrow PSF widths and there is a transient star source present. The error can significantly reduce, to less than 2% by increasing the number of measurements to 30% of the Nyquist sampling rate. For detector read-outs with a very clean PSF, we can reconstruct the images within 2% accuracy using only 10% measurements. We also show that CS techniques fail when the differenced image of interest is not sparse. As we can see when none of the stars experience any variation in magnitude, the resulting differenced image should all have pixel values close to zero. This results in a non-sparse image. Furthermore, we show that this novel CS based architecture eliminates the need to find a sparse transformation domain, while reconstructing only the needed information to

TABLE III
AVERAGE % ERROR IN MAGNITUDE OF THE SOURCE STAR AND STANDARD DEVIATION OF ERROR OVER 100 MONTE CARLO SIMULATIONS.
OBSERVED IMAGE PSF = 0.3
REFERENCE IMAGE PSF = 0.1.

Magnification Factor	Average % error (m = 0.1*n, m = 0.3*n)	standard deviation of error (m = 0.1*n, m = 0.3*n)
1	100+, 100+	2.6 x 10^8, $4.86x10^8$
1.2	7.2, 1.76	0.037, 0.0041
1.4	6.2, 0.78	0.099, 0.0017
1.6	4.1, 0.49	0.018, 0.0013
1.8	4.0, 0.28	0.0197, 0.0012

TABLE IV
AVERAGE % ERROR IN MAGNITUDE OF THE SOURCE STAR AND STANDARD DEVIATION OF ERROR OVER 100 MONTE CARLO SIMULATIONS.
NUMBER OF MEASUREMENTS IS 10% OF N AND 50% OF N, WHERE N = 128
OBSERVED IMAGE PSF = 0.5
REFERENCE IMAGE PSF = 0.1

Magnification Factor	Average % error (m = 0.1*n, m = 0.5*n)	standard deviation of error (m = 0.1*n, m = 0.5*n)
1	100+, 100+	14751, 3416
1.2	87.06, 75.13	0.26, 0.38
1.4	47.59, 28.23	0.36, 0.30
1.6	32.13, 15.17	0.22, 0.19
1.8	33.34, 8.96	0.17, 0.13

TABLE V
LEGEND DESCRIPTIONS FOR PLOTS IN FIGURE 8

Marker Name	Table Reference	Description
r1	Table I	Convolution Kernel is known 10% of Nyquist rate measurements used Observed image PSF = 0.3 Reference image PSF = 0.1
r2	Table II	Convolution Kernel is unknown 10% of Nyquist rate measurements used Observed image PSF = 0.1 Reference image PSF = 0.1
r3a	Table III	Convolution Kernel is unknown 10% of Nyquist rate measurements used Observed image PSF = 0.3 Reference image PSF = 0.1
r3b	Table III	Convolution Kernel is unknown 30% of Nyquist rate measurements used Observed image PSF = 0.3 Reference image PSF = 0.1
r4a	Table IV	Convolution Kernel is unknown 10% of Nyquist rate measurements used Observed image PSF = 0.5 Reference image PSF = 0.1
r4b	Table IV	Convolution Kernel is unknown 50% of Nyquist rate measurements used Observed image PSF = 0.5 Reference image PSF = 0.1

do transient photometric science.

VII. CONCLUSIONS

To summarize, this study shows promising results for applying CS on crowded star fields to detect and characterize transient events, such as the ones produced through gravitational microlensing. This could be a game-changing technology in the way we acquire data to efficiently capture and reconstruct samples which are of importance to science, while discarding wasteful samples. This process significantly reduces the onboard storage, power, and transmission requirements. The results of this study show that for a crowded star field with clean seeing, we need to acquire only 10% of the Nyquist rate samples to correctly capture a change in star magnitude over time. There is a trade-off with the % of measurements required and the accuracy in reconstruction, which can be studied as applicable to each science need. Further study in differencing algorithms for measurement vectors obtained through CS will produce even better results in CS reconstruction of the differenced images.

REFERENCES

[1] Seager, Sara."Exoplanets." Exoplanets (2010).
[2] Bramich, D. M."A new algorithm for difference image analysis." Monthly Notices of the Royal Astronomical Society: Letters 386.1 (2008): L77-L81.
[3] Eldar, Yonina C., and Gitta Kutyniok, eds. Compressed sensing: theory and applications. Cambridge university press, 2012.
[4] Cands, Emmanuel J., and Michael B. Wakin. "An introduction to compressive sampling [a sensing/sampling paradigm that goes against the common knowledge in data acquisition]." IEEE signal processing magazine 25.2 (2008): 21-30.
[5] Candes, Emmanuel, and Justin Romberg."Sparsity and incoherence in compressive sampling." Inverse problems 23.3 (2007): 969.
[6] Wakin, Michael B., et al."An architecture for compressive imaging." 2006 International Conference on Image Processing. IEEE, 2006.
[7] Pope, Graeme. Compressive sensing: A summary of reconstruction algorithms. MS thesis. ETH, Swiss Federal Institute of Technology Zurich, Department of Computer Science, 2009.
[8] Diamond, Steven, and Stephen Boyd."CVXPY: A Python-embedded modeling language for convex optimization." The Journal of Machine Learning Research 17.1 (2016): 2909-2913.
[9] ODonoghue, Brendan, et al."Conic optimization via operator splitting and homogeneous self-dual embedding." Journal of Optimization Theory and Applications 169.3 (2016): 1042-1068.
[10] Korde-Patel, Asmita, Richard K. Barry, and Tinoosh Mohsenin. "Application of Compressive Sensing to Gravitational Microlensing Data and Implications for Miniaturized Space Observatories." (2016).
[11] Korde-Patel, Asmita, Richard K. Barry, and Tinoosh Mohsenin."Application of Compressive Sensing to Gravitational Microlensing Experiments." Proceedings of the International Astronomical Union 12.S325 (2016): 67-70.
[12] Starck, Jean-Luc, Fionn Murtagh, and Jalal M. Fadili. Sparse image and signal processing: wavelets, curvelets, morphological diversity. Cambridge university press, 2010.
[13] Rebollo-Neira, Laura, and James Bowley. "Sparse representation of astronomical images." JOSA A 30.4 (2013): 758-768.